Fermi National Accelerator Laboratory

FERMILAB-Conf-97/158-T

Neutrino Interaction Cross Sections

Chris Quigg

Fermi National Accelerator Laboratory
P.O. Box 500, Batavia, Illinois 60510 USA
and
Department of Physics, Princeton University
Princeton, New Jersey 08540 USA

Abstract

Ultrahigh-energy neutrinos can be detected by observing long-range muons produced in charged-current neutrino-nucleon interactions. To estimate the event rates in detectors on Earth, we require predictions of neutrino fluxes from atmospheric and extraterrestrial sources and a knowledge of the interactions of neutrinos with ordinary matter. Among conventional processes, the reactions $\nu_\ell N \to \ell +$ anything and $\nu_\ell N \to \nu_\ell +$ anything are the major sources of both the desired signal and the attenuation of the neutrino "beam" *en route* to the detector.

I report new calculations of the cross sections for deeply inelastic scattering of neutrinos from isoscalar nucleons at neutrino energies between 10^9 eV and 10^{21} eV. I compare with results in the literature and assess the reliability of current predictions. For completeness, I briefly survey the cross sections for neutrino interactions with atomic electrons, emphasizing the role of the W-boson resonance in $\bar{\nu}_e e$ interactions for neutrino energies in the neighborhood of 6.3 PeV.

Unconventional processes could provide new signals for ultrahigh-energy neutrino interactions, and would alter the attenuation length of UHE neutrinos. As an example, I discuss the scalar leptoquark and R-parity-violating squark interpretations of the high-Q^2 anomaly reported by the H1 and ZEUS Collaborations working at the electron-proton collider HERA.

Operated by Universities Research Association Inc. under Contract No. DE-AC02-76CH03000 with the United States Department of Energy

Disclaimer

Distribution

Approved for public release: further dissemination unlimited.

Neutrino Interaction Cross Sections

Chris Quigg
quigg@fnal.gov
Fermilab and Princeton

- Issues in the prediction of νN cross sections
- New calculations of $\sigma(\nu_\ell N \to \ell + \text{anything})$ and $\sigma(\nu_\ell N \to \nu_\ell + \text{anything})$, using CTEQ4 parton distributions
- Review of $\bar{\nu}_e e$ interactions on the W^- resonance near 6.3 PeV
- Implications of the HERA high-Q^2 anomaly

R. Gandhi, C. Quigg, M. H. Reno, and I. Sarcevic, *Astroparticle Physics* **5**, 81 (1996).

Slide 1

Interaction length of a 1-GeV ν is

$$\mathcal{L}_{\rm int} \equiv \frac{1}{\sigma \cdot N_A} = 2.5 \times 10^9 \text{ kmwe}$$
$$= \tfrac{1}{4} \times 10^9 \text{ t/cm}^2$$
$$\approx 2.3 \text{ light-hours w.e.}$$

LONG!

- Possibility of filtered neutrino beams
- Missing-energy signature for neutrinos
- Neutrinos can bring information from processes otherwise obscured by a few hundred grams of material
- Difficulty of detecting neutrino interactions

Slide 2

$\mathcal{L}_{\rm int}$ decreases with increasing energy

(mirrors the rise of the cross section)

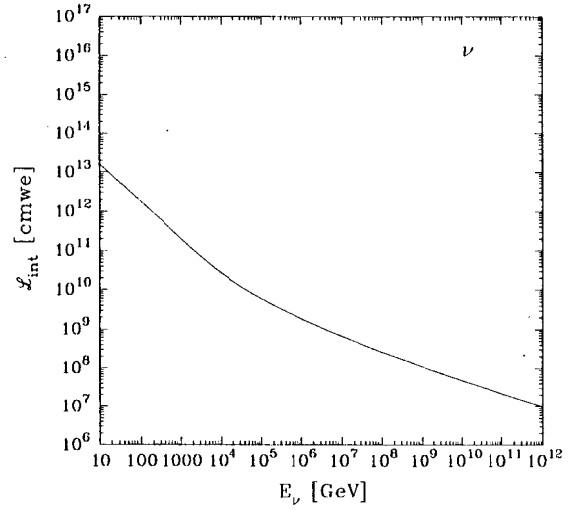

Earth diameter	1.1×10^{10} cmwe $= 11$ kt/cm^2
Atmosphere	$\approx 10^3$ cmwe vertical $\approx 3.6 \times 10^4$ cmwe horizontal

Slide 3

Material encountered by an upward-going ν
(Preliminary Reference Earth Model)

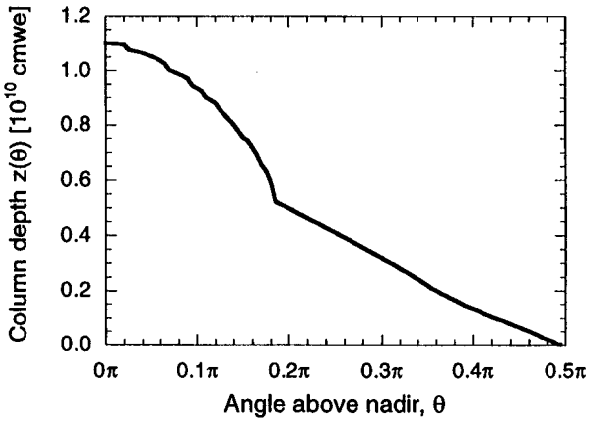

Influence of Earth's core visible at angles $< 0.2\pi$
Diameter opaque to neutrinos above 40 TeV

Slide 4

$\nu_\mu N \to \mu^- + \text{anything}$

$$\frac{d^2\sigma}{dxdy} = \frac{2G_F^2 M E_\nu}{\pi}\left(\frac{M_W^2}{Q^2+M_W^2}\right)^2\left[xq(x,Q^2)+x\bar{q}(x,Q^2)(1-y)^2\right]$$

Quark distribution functions are

$$q(x,Q^2) = \frac{u_v(x,Q^2)+d_v(x,Q^2)}{2}+\frac{u_s(x,Q^2)+d_s(x,Q^2)}{2} + s_s(x,Q^2)+b_s(x,Q^2)$$

$$\bar{q}(x,Q^2) = \frac{u_s(x,Q^2)+d_s(x,Q^2)}{2}+c_s(x,Q^2)+t_s(x,Q^2),$$

Modern parton distribution functions (PDFs) are derived from fits to a vast universe of data.

Isoscalar nucleon: $N \equiv \frac{n+p}{2}$;
$x = Q^2/2M\nu$; $y = \nu/E_\nu$;
$\nu = E_\nu - E_\mu$: energy loss in the lab (target) frame;
M and M_W: nucleon and intermediate-boson masses;
$G_F = 1.16632 \times 10^{-5}$ GeV^{-2}: Fermi constant.

Slide 5

Andreev, Berezinsky, Smirnov (1979):

At high neutrino energies,

$\left(\frac{M_W^2}{Q^2+M_W^2}\right)^2$ limits $Q^2 = 2ME_\nu xy \lesssim M_W^2$,

and so limits effective interval in x to

$$x \lesssim M_W^2/2ME_\nu.$$

- Damping *diminishes* σ below the point-coupling, parton-model value. Cross section grows less rapidly than E_ν^1.
- QCD evolution (growth of small-x parton densities with increasing Q^2) *enhances* σ.

Slide 6

Q^2-evolution of parton distributions

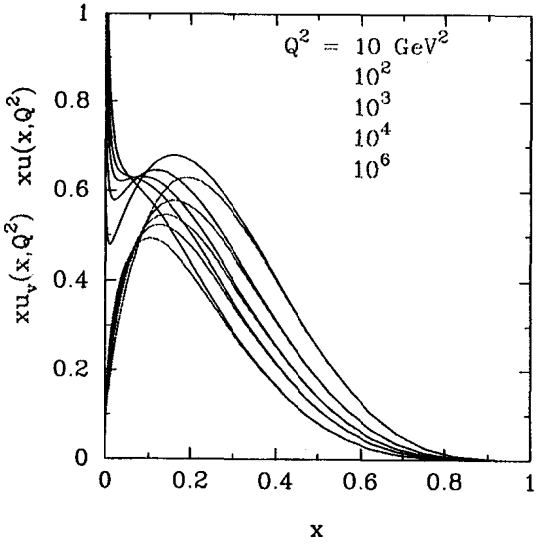

CTEQ4M

Slide 7

Need to:

- Determine parton distributions at

$$x \lesssim 10^{-4}, \quad Q^2 \approx 10^4 \text{ GeV}^2$$

where they have not been measured.

- Include heavy flavors

Done for the first time in EHLQ (1984) structure functions developed for SSC physics applications, which required

$$x \gtrsim 10^{-4}, \quad Q^2 \lesssim 10^8 \text{ GeV}^2.$$

Slide 8

Evolution of flavors in the proton

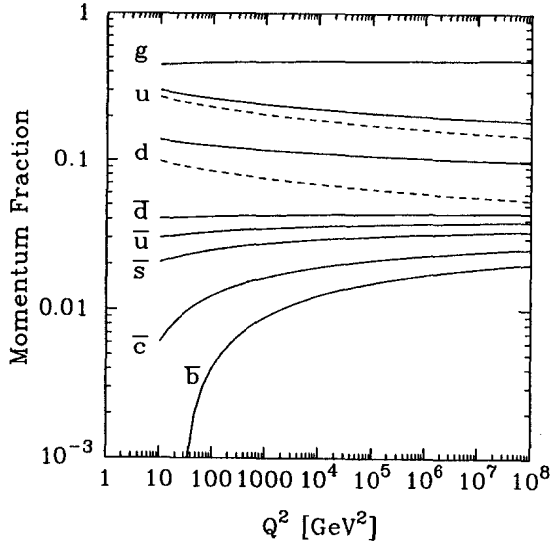

6 quark flavors, $Q^2 \to \infty$:

momentum fraction in gluons is $G_2^\infty = 8/17$;
each q, $\bar{q}$ species carries $\bar{q}_2^\infty = 3/68$.

Slide 9

Very small values of x encountered at ultrahigh energies enter régime in which standard Altarelli–Parisi evolution is inadequate ($\log 1/x$ as well as $\log Q^2$) ...

... and approach régime in which parton-model incoherence breaks down (high density of partons).

For $x < 10^{-4}$, QRW86 used double-log approximation* (DLA) of Gribov, Levin, Ryskin:

$$xq_s(x,Q^2) = C(Q^2)\sqrt{\frac{2(\xi-\xi_0)}{\rho}}\exp\{\left[(2\rho(\xi-\xi_0)\right]^{1/2}\},$$

a summation of the most singular contributions to parton distributions.

$\rho = (8N/b_0)\ln(1/x)$, $\xi(Q) = \ln\ln(Q^2/\Lambda^2)$, $N = 3$ is the number of colors, and $b_0 = (11N - 2n_f)/3$ for n_f flavors.

---

* *Cf.* McKay & Ralston 86.

Slide 10

More singular parton distributions (and a rapid Q^2-dependence) are generated dynamically by the Balitskiĭ–Fadin–Kuraev–Lipatov approach, a leading $\alpha_s \log 1/x$ resummation of soft gluon emissions:

$$xq_s(x,Q^2) \sim \sqrt{Q^2}\, x^{-0.5}.$$

Most contemporary PDFs feature singular behavior at $x \to 0$, though not so dramatic as BFKL.

$$xq_s(x) \propto x^{-\lambda} \text{ as } x \to 0,$$

CTEQ4	$\lambda = 0.227$
CTEQ3	$\lambda \approx 0.28$ to 0.35
MRSA′	$\lambda = 0.17$
MRSG	$\lambda_s = 0.067$, $\lambda_g = 0.301$
MRSD_’	$\lambda = 0.5$

Slide 11

Uncertainties at small x

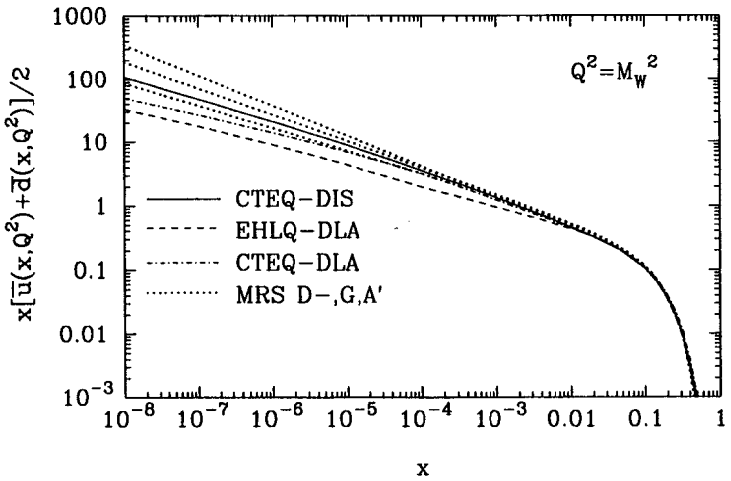

Slide 12

CTEQ4D at small x

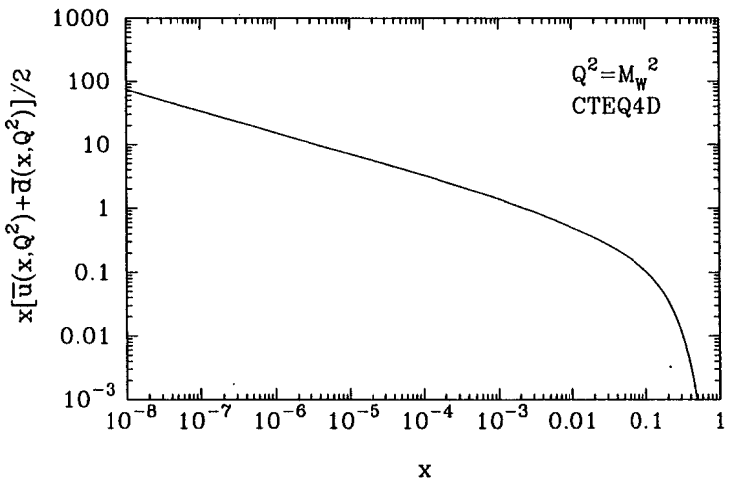

H. L. Lai, *et al.*, *Phys. Rev.* **D55**, 1280 (1997).

Slide 13

Flavor Components of σ_{cc}

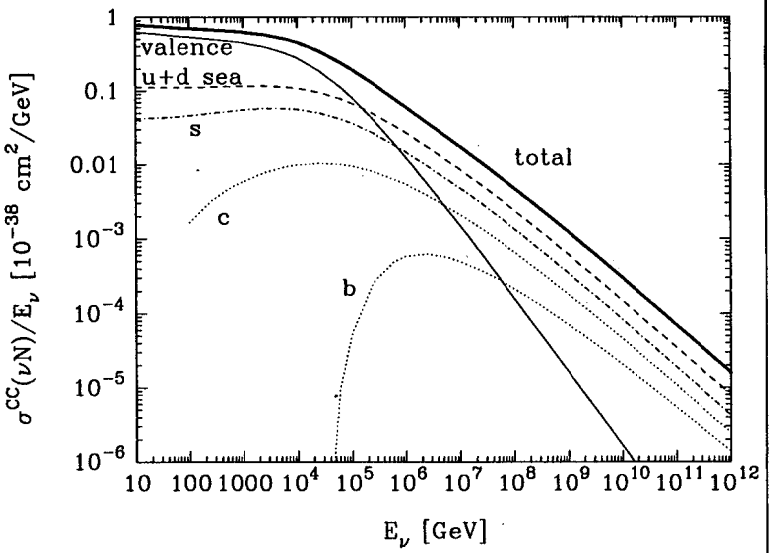

CTEQ3

Slide 14

The importance of small x

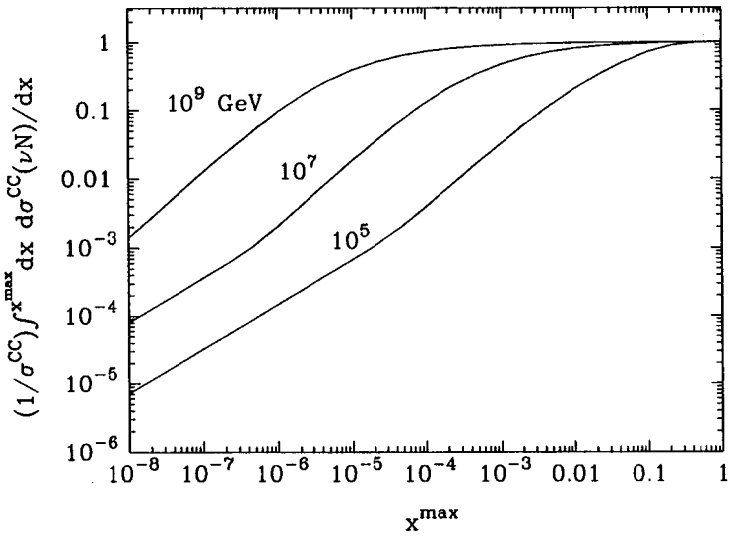

Slide 15

The importance of small x

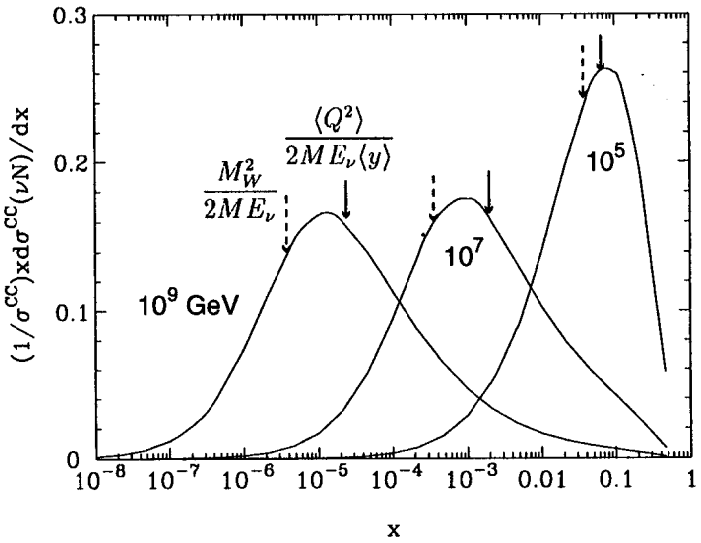

Slide 16

Evolution increases cross section
by 20× at 10^{10} GeV.

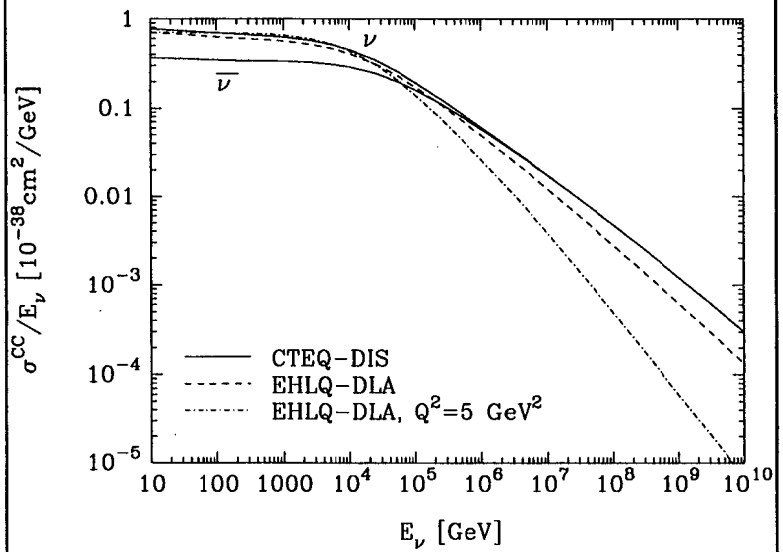

CTEQ3

Slide 17

GQRS96

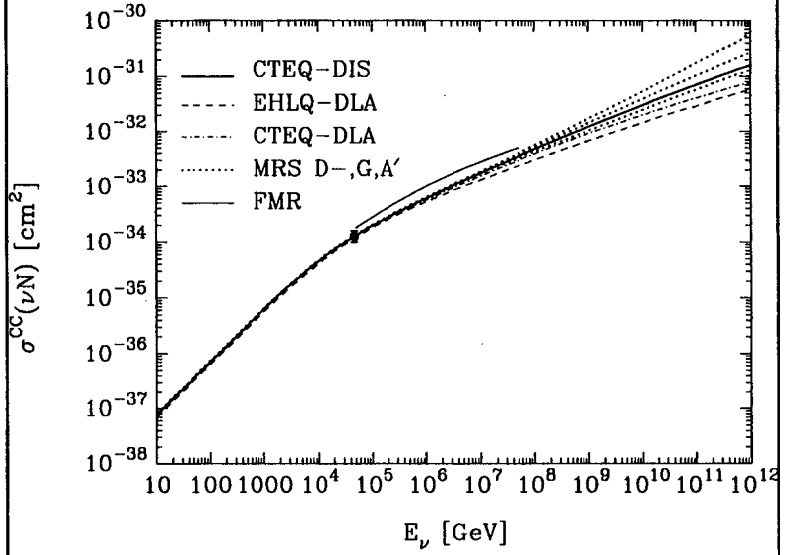

Slide 18

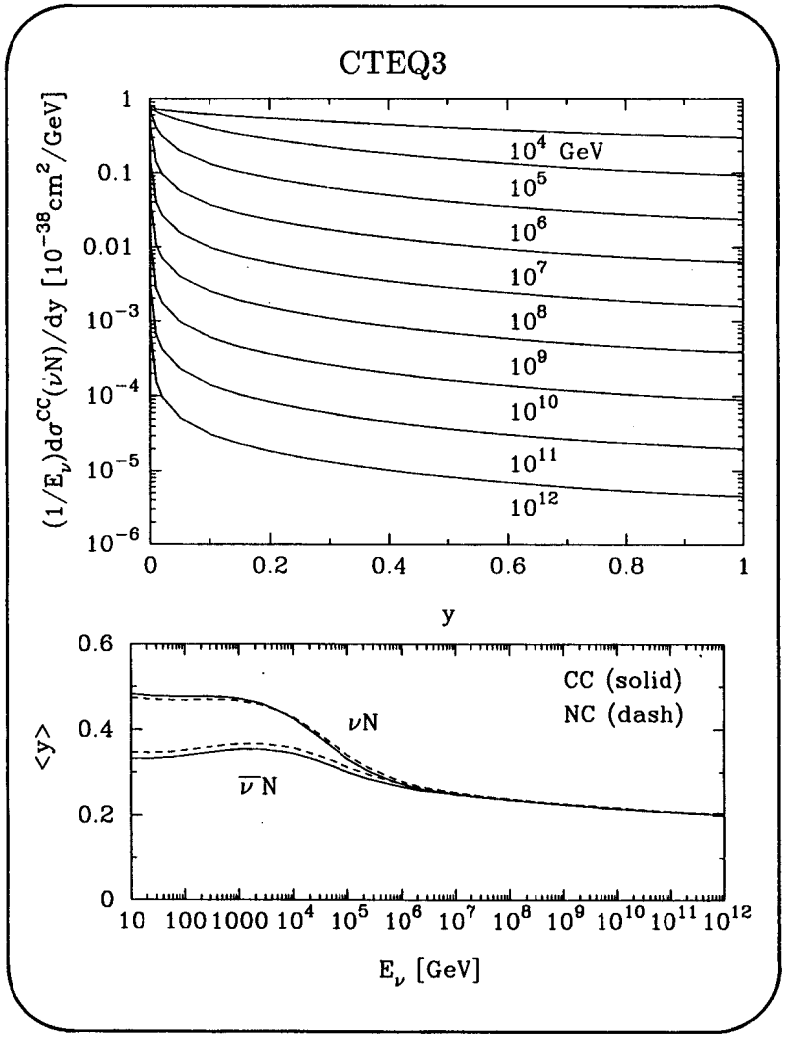

Slide 19

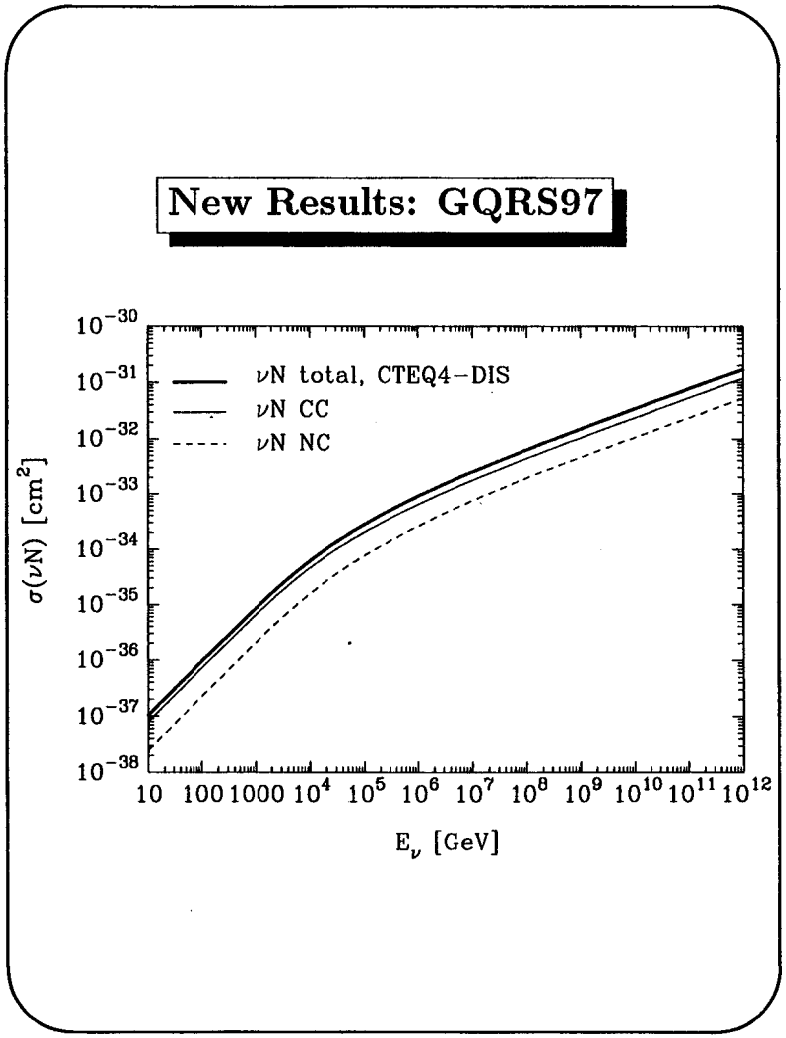

Slide 20

New Results: GQRS97

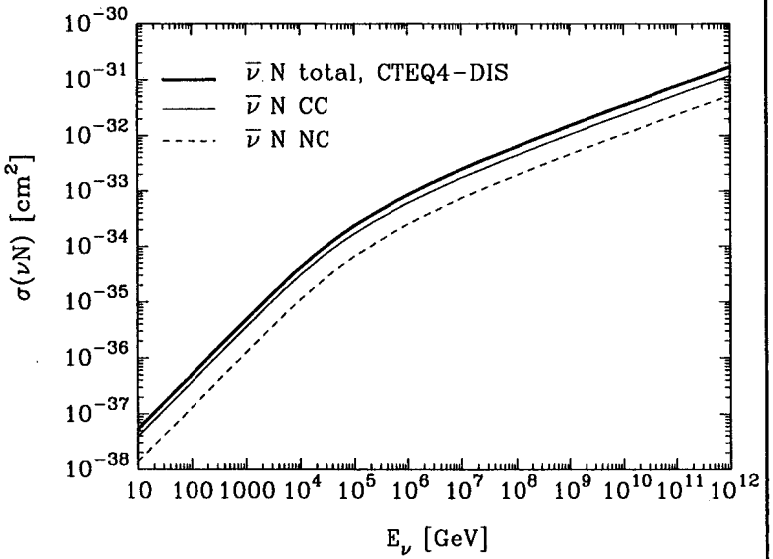

Slide 21

Compare CTEQ3

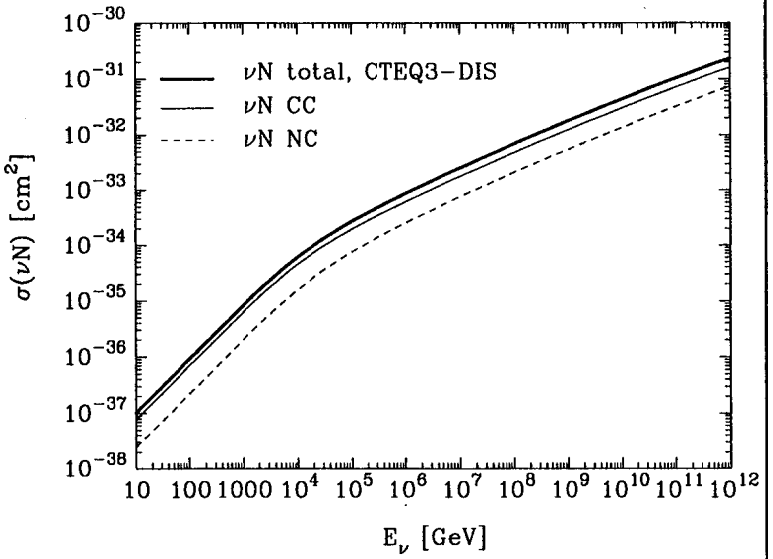

Slide 22

Comparison with GQRS96

CTEQ4 less singular than GQRS96 PDFs.

$$xq_s(x) \propto x^{-\lambda} \text{ as } x \to 0,$$

CTEQ4D	$\lambda = 0.227$
CTEQ3D	$\lambda = 0.332$

$\Longrightarrow$ smaller cross section at highest energies.

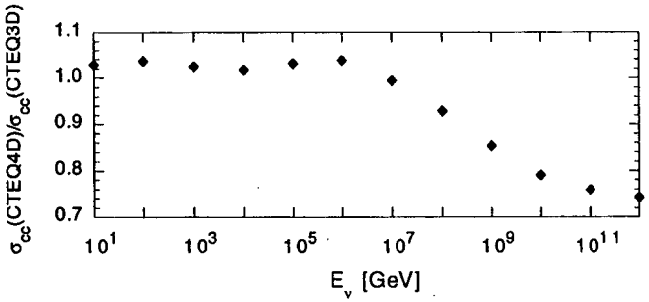

Slide 23

More glue at large x has little effect

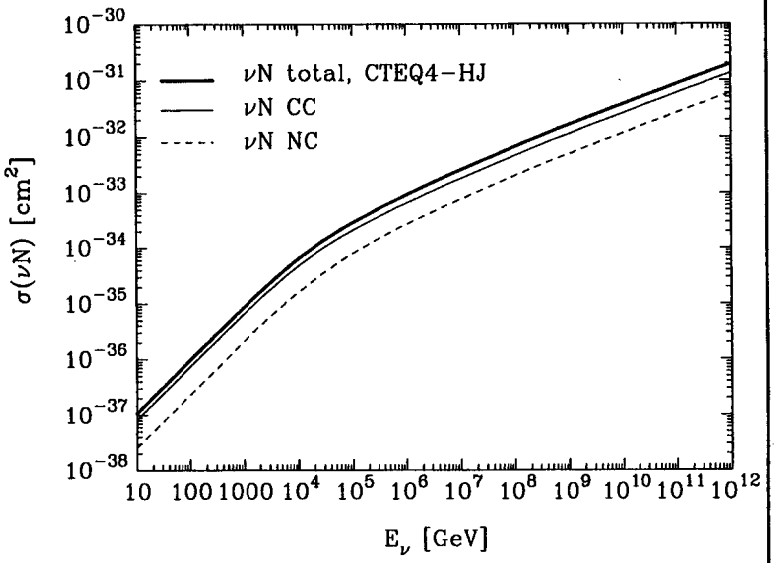

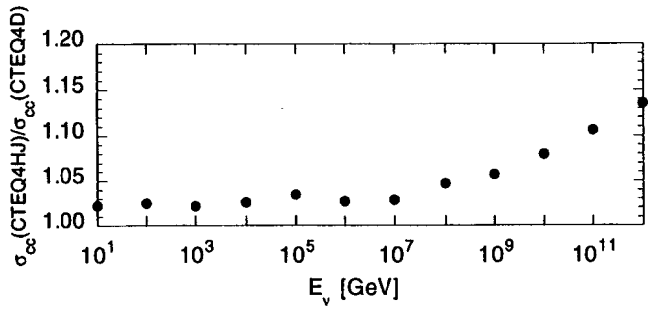

Slide 24

Over a broad range of Q^2, HERA data agree with electroweak theory and standard (MRSD_') parton distributions.

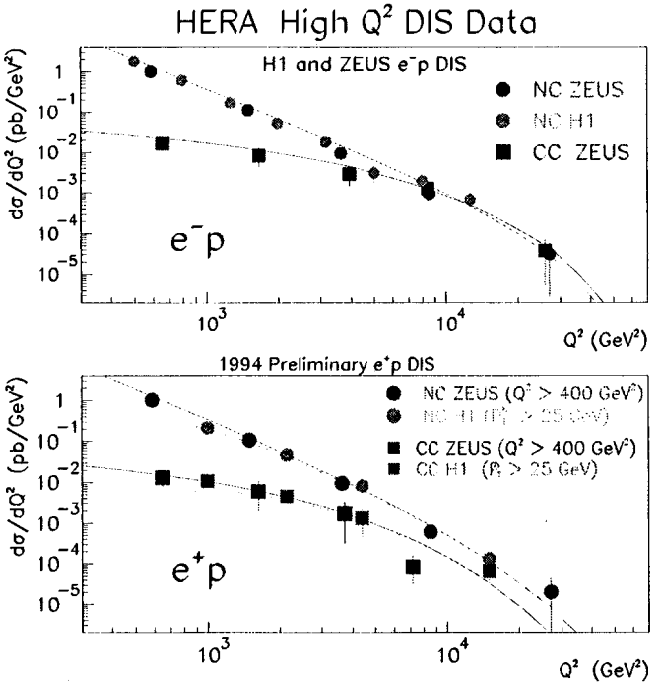

Slide 25

Other Recent Calculations of UHE νN Cross Sections

Author (year)	Parton Distributions
Hill (97)*	MRSG, FMR
GQRS (96)	CTEQ3, MRSD_,G,A′
Parente & Zas (95)	MRSG
Butkevich, *et al.* (95)	MRSA, GRV92, MT
Frichter, McKay, Ralston (95)	FMR
Butkevich, *et al.* (88)	GHR–DLA
Quigg, Reno, Walker (86) Reno & Quigg (88)	EHLQ–DLA
McKay & Ralston	DLA

* *Astroparticle Physics* **6**, 215 (1997).

Table 1: Charged-current and neutral-current cross sections for νN interactions, and the corresponding values of the mean inelasticity $\langle y \rangle$, for the CTEQ3-DIS distributions. [From GQRS96]

E_ν [GeV]	σ_{CC} [cm^2]	σ_{NC} [cm^2]	$\langle y \rangle_{CC}$	$\langle y \rangle_{NC}$
10^1	0.777×10^{-37}	0.242×10^{-37}	0.483	0.474
10^2	0.697×10^{-36}	0.217×10^{-36}	0.477	0.470
10^3	0.625×10^{-35}	0.199×10^{-35}	0.472	0.467
10^4	0.454×10^{-34}	0.155×10^{-34}	0.426	0.428
10^5	0.196×10^{-33}	0.745×10^{-34}	0.332	0.341
10^6	0.611×10^{-33}	0.252×10^{-33}	0.273	0.279
10^7	0.176×10^{-32}	0.748×10^{-33}	0.250	0.254
10^8	0.478×10^{-32}	0.207×10^{-32}	0.237	0.239
10^9	0.123×10^{-31}	0.540×10^{-32}	0.225	0.227
10^{10}	0.301×10^{-31}	0.134×10^{-31}	0.216	0.217
10^{11}	0.706×10^{-31}	0.316×10^{-31}	0.208	0.210
10^{12}	0.159×10^{-30}	0.715×10^{-31}	0.205	0.207

Table 2: Charged-current and neutral-current cross sections for $\bar{\nu} N$ interactions, and the corresponding values of the mean inelasticity $\langle y \rangle$, for the CTEQ3-DIS distributions. [From GQRS96]

E_ν [GeV]	σ_{CC} [cm^2]	σ_{NC} [cm^2]	$\langle y \rangle_{CC}$	$\langle y \rangle_{NC}$
10^1	0.368×10^{-37}	0.130×10^{-37}	0.333	0.350
10^2	0.349×10^{-36}	0.122×10^{-36}	0.340	0.354
10^3	0.338×10^{-35}	0.120×10^{-35}	0.354	0.368
10^4	0.292×10^{-34}	0.106×10^{-34}	0.345	0.358
10^5	0.162×10^{-33}	0.631×10^{-34}	0.301	0.313
10^6	0.582×10^{-33}	0.241×10^{-33}	0.266	0.273
10^7	0.174×10^{-32}	0.742×10^{-33}	0.249	0.253
10^8	0.477×10^{-32}	0.207×10^{-32}	0.237	0.239
10^9	0.123×10^{-31}	0.540×10^{-32}	0.225	0.227
10^{10}	0.301×10^{-31}	0.134×10^{-31}	0.216	0.217
10^{11}	0.706×10^{-31}	0.316×10^{-31}	0.208	0.210
10^{12}	0.159×10^{-30}	0.715×10^{-31}	0.205	0.207

Table 3: Charged-current and neutral-current cross sections and their sum for νN interactions according to the CTEQ4-DIS distributions.

E_ν GeV	$\sigma_{\rm CC}$ [cm^2]	$\sigma_{\rm NC}$ [cm^2]	$\sigma_{\rm tot}$ [cm^2]
10^1	0.799×10^{-37}	0.249×10^{-37}	0.105×10^{-36}
10^2	0.722×10^{-36}	0.226×10^{-36}	0.948×10^{-36}
10^3	0.640×10^{-35}	0.204×10^{-35}	0.844×10^{-35}
10^4	0.462×10^{-34}	0.158×10^{-34}	0.619×10^{-34}
10^5	0.202×10^{-33}	0.767×10^{-34}	0.279×10^{-33}
10^6	0.634×10^{-33}	0.260×10^{-33}	0.894×10^{-33}
10^7	0.175×10^{-32}	0.748×10^{-33}	0.250×10^{-32}
10^8	0.444×10^{-32}	0.194×10^{-32}	0.638×10^{-32}
10^9	0.105×10^{-31}	0.464×10^{-32}	0.151×10^{-31}
10^{10}	0.238×10^{-31}	0.107×10^{-31}	0.345×10^{-31}
10^{11}	0.536×10^{-31}	0.238×10^{-31}	0.773×10^{-31}
10^{12}	0.118×10^{-30}	0.520×10^{-31}	0.170×10^{-30}

Table 4: Charged-current and neutral-current cross sections and their sum for $\bar{\nu} N$ interactions according to the CTEQ4-DIS distributions.

E_ν GeV	$\sigma_{\rm CC}$ [cm^2]	$\sigma_{\rm NC}$ [cm^2]	$\sigma_{\rm tot}$ [cm^2]
10^1	0.394×10^{-37}	0.138×10^{-37}	0.532×10^{-37}
10^2	0.375×10^{-36}	0.131×10^{-36}	0.505×10^{-36}
10^3	0.354×10^{-35}	0.124×10^{-35}	0.479×10^{-35}
10^4	0.301×10^{-34}	0.109×10^{-34}	0.410×10^{-34}
10^5	0.168×10^{-33}	0.652×10^{-34}	0.233×10^{-33}
10^6	0.605×10^{-33}	0.249×10^{-33}	0.854×10^{-33}
10^7	0.173×10^{-32}	0.742×10^{-33}	0.248×10^{-32}
10^8	0.443×10^{-32}	0.194×10^{-32}	0.637×10^{-32}
10^9	0.105×10^{-31}	0.464×10^{-32}	0.151×10^{-31}
10^{10}	0.241×10^{-31}	0.107×10^{-31}	0.347×10^{-31}
10^{11}	0.534×10^{-31}	0.238×10^{-31}	0.771×10^{-31}
10^{12}	0.117×10^{-30}	0.520×10^{-31}	0.169×10^{-30}

Table 5: Charged-current and neutral-current cross sections and their sum for νN interactions according to the CTEQ4-HJ distributions.

E_ν GeV	σ_{CC} [cm^2]	σ_{NC} [cm^2]	σ_{tot} [cm^2]
10^1	0.817×10^{-37}	0.255×10^{-37}	0.107×10^{-36}
10^2	0.740×10^{-36}	0.231×10^{-36}	0.971×10^{-36}
10^3	0.654×10^{-35}	0.208×10^{-35}	0.862×10^{-35}
10^4	0.474×10^{-34}	0.161×10^{-34}	0.635×10^{-34}
10^5	0.209×10^{-33}	0.789×10^{-34}	0.287×10^{-33}
10^6	0.651×10^{-33}	0.267×10^{-33}	0.918×10^{-33}
10^7	0.180×10^{-32}	0.771×10^{-33}	0.257×10^{-32}
10^8	0.465×10^{-32}	0.204×10^{-32}	0.668×10^{-32}
10^9	0.111×10^{-31}	0.493×10^{-32}	0.161×10^{-31}
10^{10}	0.257×10^{-31}	0.115×10^{-31}	0.372×10^{-31}
10^{11}	0.593×10^{-31}	0.264×10^{-31}	0.857×10^{-31}
10^{12}	0.134×10^{-30}	0.594×10^{-31}	0.193×10^{-30}

Table 6: Charged-current and neutral-current cross sections and their sum for $\bar{\nu}N$ interactions according to the CTEQ4-HJ distributions.

E_ν GeV	σ_{CC} [cm^2]	σ_{NC} [cm^2]	σ_{tot} [cm^2]
10^1	0.412×10^{-37}	0.144×10^{-37}	0.555×10^{-37}
10^2	0.392×10^{-36}	0.136×10^{-36}	0.528×10^{-36}
10^3	0.367×10^{-35}	0.128×10^{-35}	0.495×10^{-35}
10^4	0.311×10^{-34}	0.112×10^{-34}	0.423×10^{-34}
10^5	0.174×10^{-33}	0.670×10^{-34}	0.241×10^{-33}
10^6	0.622×10^{-33}	0.256×10^{-33}	0.878×10^{-33}
10^7	0.179×10^{-32}	0.765×10^{-33}	0.255×10^{-32}
10^8	0.462×10^{-32}	0.203×10^{-32}	0.665×10^{-32}
10^9	0.112×10^{-31}	0.493×10^{-32}	0.161×10^{-31}
10^{10}	0.261×10^{-31}	0.115×10^{-31}	0.375×10^{-31}
10^{11}	0.590×10^{-31}	0.264×10^{-31}	0.854×10^{-31}
10^{12}	0.132×10^{-30}	0.594×10^{-31}	0.192×10^{-30}

Power-Law Parametrizations

For 10^{16} eV $\leq E_\nu \leq 10^{21}$ eV, the CTEQ4–DIS cross sections are given within 10% by

$$\sigma_{\rm CC}(\nu N) = 5.53 \times 10^{-36}\ {\rm cm}^2 \left(\frac{E_\nu}{1\ {\rm GeV}}\right)^{0.363}$$

$$\sigma_{\rm NC}(\nu N) = 2.31 \times 10^{-36}\ {\rm cm}^2 \left(\frac{E_\nu}{1\ {\rm GeV}}\right)^{0.363}$$

$$\sigma_{\rm tot}(\nu N) = 7.84 \times 10^{-36}\ {\rm cm}^2 \left(\frac{E_\nu}{1\ {\rm GeV}}\right)^{0.363}$$

$$\sigma_{\rm CC}(\bar{\nu} N) = 5.52 \times 10^{-36}\ {\rm cm}^2 \left(\frac{E_\nu}{1\ {\rm GeV}}\right)^{0.363}$$

$$\sigma_{\rm NC}(\bar{\nu} N) = 2.29 \times 10^{-36}\ {\rm cm}^2 \left(\frac{E_\nu}{1\ {\rm GeV}}\right)^{0.363}$$

$$\sigma_{\rm tot}(\bar{\nu} N) = 7.80 \times 10^{-36}\ {\rm cm}^2 \left(\frac{E_\nu}{1\ {\rm GeV}}\right)^{0.363}$$

Slide 26

Assessment

How well can we predict $\sigma(\nu_\ell N \to \ell + \text{anything})$ and $\sigma(\nu_\ell N \to \nu_\ell + \text{anything})$?

- For $E_\nu \lesssim 10^{16}$ eV, all standard PDFs yield very similar cross sections.
- For $E_\nu \gtrsim 10^{16}$ eV, cross sections are sensitive to PDFs at very small x, where there are no direct experimental constraints.
- Different *assumptions* about $x \to 0$ behavior then lead to different cross sections.
- At 10^{20} eV, uncertainty reaches a factor $2^{\pm 1}$.

Slide 27

νe Scattering

- m_e is small: $\sigma(\nu e) \ll \sigma(\nu N)$ at almost all energies.
- Exception: resonant $\bar{\nu}_e e \to W^-$ formation.
- At resonance ($E_\nu = 6.3$ PeV), $\sigma(\bar{\nu}_e e \to W^- \to \text{anything}) \approx 5 \times 10^{-31}$ cm^2, about $350 \times \sigma(\nu_\mu N \to \mu^- + \text{anything})$.

Slide 28

νe Scattering

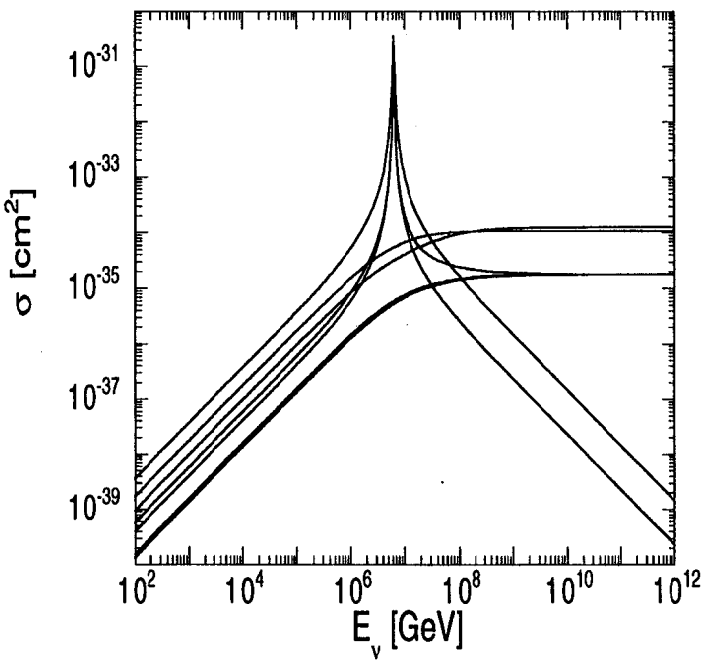

Largest to smallest at low energies: (i) $\bar{\nu}_e e \to$ hadrons, (ii) $\nu_\mu e \to \mu \nu_e$, (iii) $\nu_e e \to \nu_e e$, (iv) $\bar{\nu}_e e \to \bar{\nu}_\mu \mu$, (v) $\bar{\nu}_e e \to \bar{\nu}_e e$, (vi) $\nu_\mu e \to \nu_\mu e$, (vii) $\bar{\nu}_\mu e \to \bar{\nu}_\mu e$.

Slide 29

GQRS97

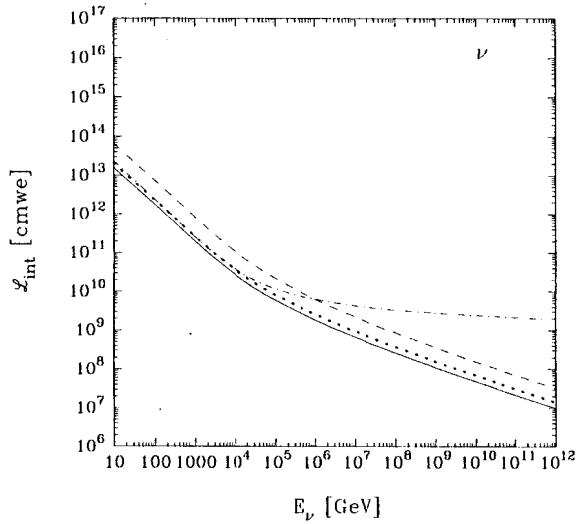

CTEQ4D

Slide 30

GQRS97

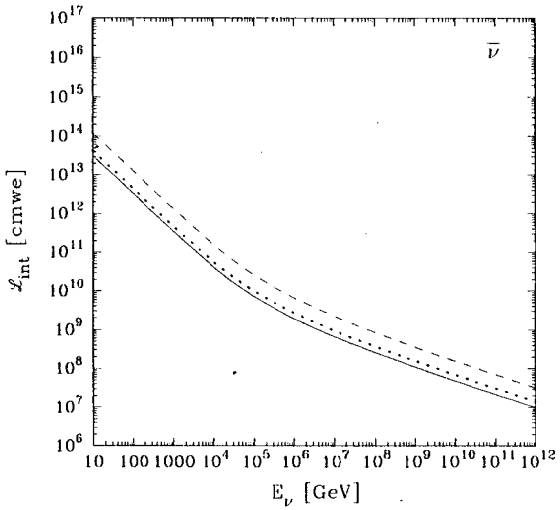

CTEQ4D

Slide 31

$$\mathcal{L}_{\rm int}^{(e)} \equiv \frac{1}{\sigma_{\nu e} \cdot (10/18) \cdot N_A}$$

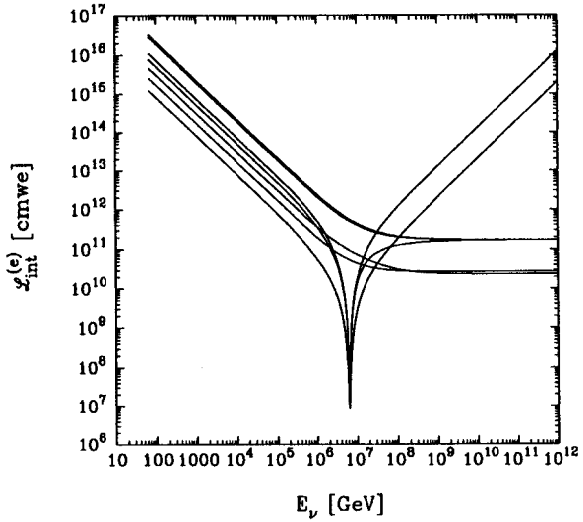

Smallest to largest at low energies:

(i) $\bar{\nu}_e e \to$ hadrons, (ii) $\nu_\mu e \to \mu \nu_e$, (iii) $\nu_e e \to \nu_e e$,

(iv) $\bar{\nu}_e e \to \bar{\nu}_\mu \mu$, (v) $\bar{\nu}_e e \to \bar{\nu}_e e$, (vi) $\nu_\mu e \to \nu_\mu e$,

(vii) $\bar{\nu}_\mu e \to \bar{\nu}_\mu e$.

Slide 32

Astrophysical Neutrino Fluxes

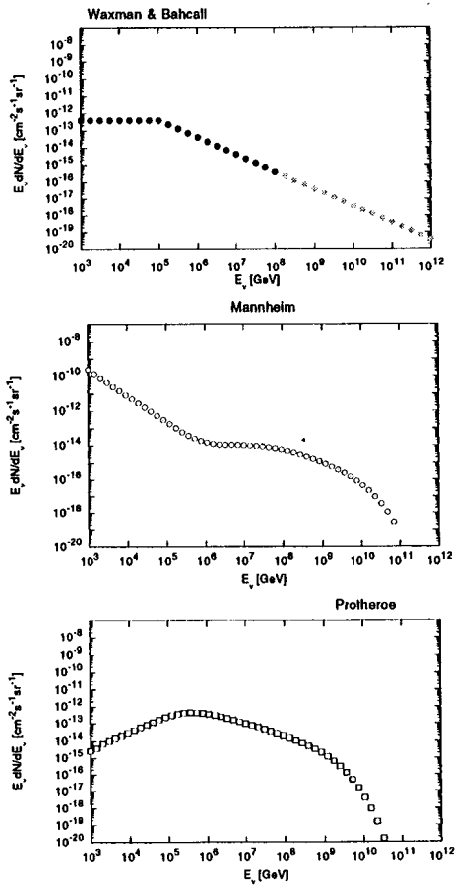

Slide 33

Event Rates, $E_\mu^{\rm min} = 1$ TeV

Upward $\mu^+ + \mu^-$ events per year arising from $\nu_\mu N$ and $\bar{\nu}_\mu N$ interactions in rock, for a detector with effective area $A = 0.1$ km^2 and muon energy threshold $E_\mu^{\rm min} = 1$ TeV.

Flux	CTEQ4D analytic	CTEQ4D LS
ATM (Stanev)	1502–1521	1225–1244
ATM (Volkova)	1093–1106	892–905
Protheroe $p\gamma$	52–65	37–46
Mannheim	32–35	25–27
Waxman–Bahcall	13–15	10–11

The smaller value of each pair corresponds to attenuation by the total cross section; the larger to attenuation by charged-current interactions.

R. J. Protheroe, astro-ph/9607165.

K. Mannheim, *Astroparticle Physics* **3**, 295 (1995).

E. Waxman & J. Bahcall, *Phys. Rev. Lett.* **78**, 2292 (1997).

Slide 34

Event Rates, $E_\mu^{\rm min} = 10$ TeV

Upward $\mu^+ + \mu^-$ events per year arising from $\nu_\mu N$ and $\bar{\nu}_\mu N$ interactions in rock, for a detector with effective area $A = 0.1$ km^2 and muon energy threshold $E_\mu^{\rm min} = 10$ TeV.

Flux	CTEQ4D analytic	CTEQ4D LS
ATM (Stanev)	26	19–20
ATM (Volkova)	20–21	14–15
Protheroe $p\gamma$	35–45	24–30
Mannheim	7–8	5–6
Waxman–Bahcall	6–8	4–5

The smaller value of each pair corresponds to attenuation by the total cross section; the larger to attenuation by charged-current interactions.

Slide 35

High Thresholds

Downward $\mu^+ + \mu^-$ events per year arising from $\nu_\mu N$ and $\bar{\nu}_\mu N$ interactions in 1 km^3 of water.

$E_\mu^{\min} =$	0.1 PeV	1 PeV	3 PeV
Mannheim 95	23	15	14
Protheroe 96	163	113	75

Slide 36

Angular Distribution

- Isotropic at $E_\nu \approx 1$ TeV
- Angles near nadir shadowed increasingly at higher energies

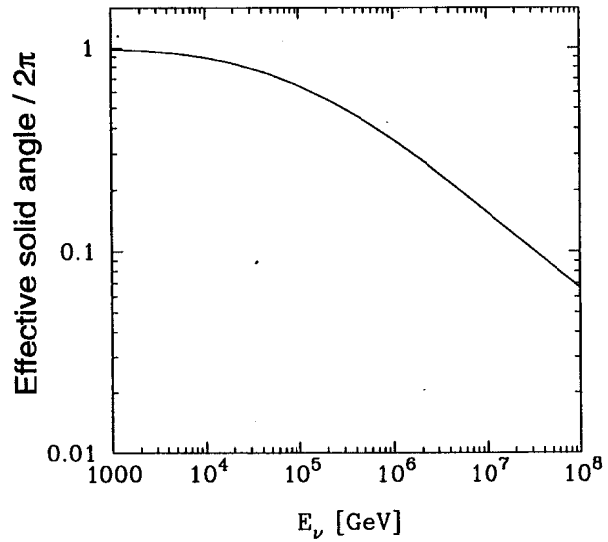

CTEQ3

Slide 37

Non-acceleration Sources

Topological Defects $\rightarrow X \rightarrow \cdots \rightarrow \nu + \ldots$

Rate of release of X particles is

$$\frac{dN_X(t)}{dt} = \kappa M_X^p t^{-4+p}$$

$p = 1$: collapse of cosmic-string loops

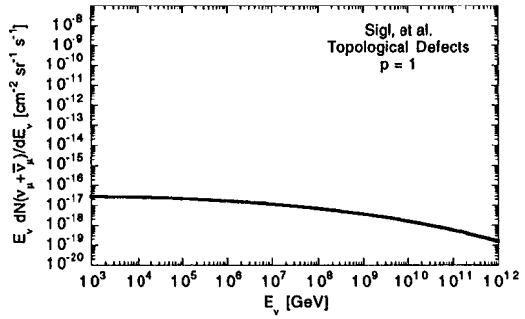

$\lesssim 0.1$ downward event/yr/km^3, $E_\mu^{\rm min} = 10^7$ GeV.

(Comparable to rates expected from CR-4 cosmic ν flux.)

G. Sigl, *et al.*, *Phys. Lett.* **B392**, 129 (1997)

Slide 38

The High-Q^2 Anomaly

The HERA experiments H1 and ZEUS have reported an excess of events at high Q^2, or high x, in the neutral-current reaction

$$e^+ p \rightarrow e^+ + \text{anything}$$

in collisions of 27.5-GeV positrons on 820-GeV protons, at $E_{\rm cm} = 300$ GeV.

No strong evidence yet about an anomaly in the charged-current reaction

$$e^+ p \rightarrow \bar{\nu}_e + \text{anything},$$

or in $e^- p$ collisions.

C. Adloff, *et al.* (H1 Collaboration), hep-ex/9702012.

J. Breitweg, *et al.* (ZEUS Collaboration), hep-ex/9702015.

Slide 39

$e^+p \to e^+ +$ anything

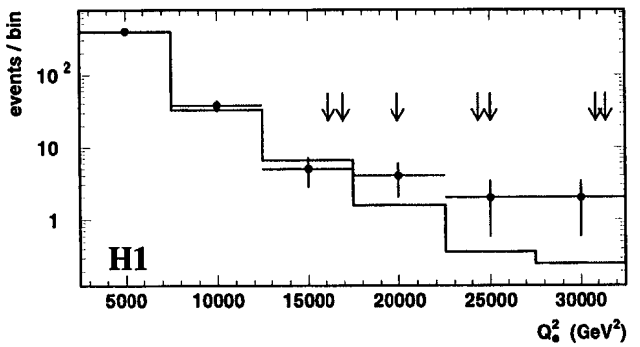

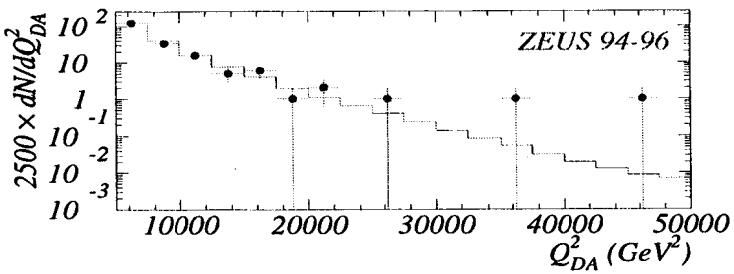

Slide 40

Possible Interpretations

- Broad Enhancement:

  Unconventional QCD evolution, or weird resummation effects.

  A small deviation from the expected $(1-x)^p$ behavior of $xq(x)$ as $x \to 1$.

  e^+q contact interaction (compositeness).

- Narrow Resonance:

  Leptoquark (e^+u or e^+d) resonance.

  $\tilde{u}$, $\tilde{c}$, or $\tilde{t}$ squark formed in R-parity-violating production and decay.

Slide 41

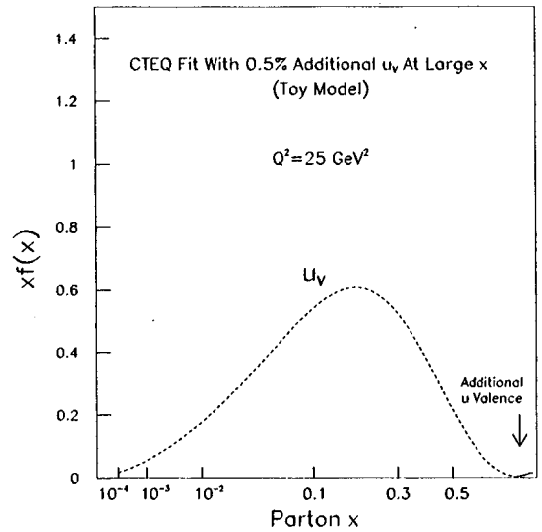

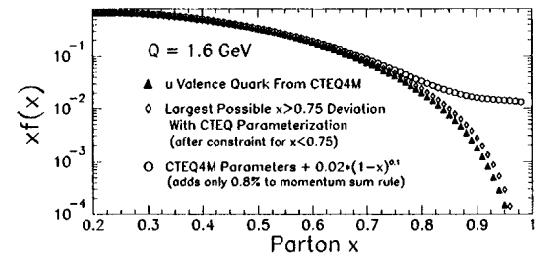

S. Kuhlman, H. L. Lai, and W. K. Tung, hep-ph/9704338.

Slide 42

Comments on New Physics

Compositeness: Broad enhancement not a good match to H1 claim of a narrow resonance.

Leptoquarks: Not supported by observations at the Tevatron Collider.

- DØ Limit: $M_{\mathrm{LQ}} \gtrsim 175$ GeV/c^2, for 100% decays into e^+q.
- CDF Limit: $M_{\mathrm{LQ}} \gtrsim 210$ GeV/c^2, for 100% decays into e^+q.

Squarks: A challenging slalom course.

- Tune spectrum so R-violating branching fraction is appreciable.
- Account for absence of $\mu^+ +$ jet signal.
- Respect bounds on $|\lambda_{ijk}|$, products of λs.

Slide 43

Resonant (scalar) LQ Formation

$$\Gamma(\mathrm{LQ}) = \frac{\lambda^2 M}{8\pi} \text{ (typically, } \lambda \ll 1).$$

Partonic cross section for resonant LQ formation:

$$\hat{\sigma}(M^2 = xs) = \frac{\pi\lambda^2}{4M^2} x\delta(x - M^2/s),$$

so that

$$\sigma(\nu p \to \mathrm{LQ}+\text{anything}) = \frac{\pi\lambda^2}{4M^2} xq(x = M^2/s, M^2).$$

Cf. R. W. Robinett, *Phys. Rev.* D**37**, 84 (1988).

Slide 44

$M_{\mathrm{LQ}} = 200$ GeV/c^2:

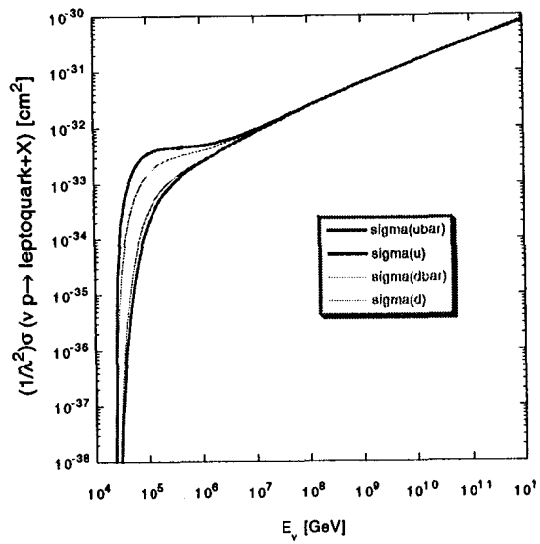

Parton momentum fraction at resonance:

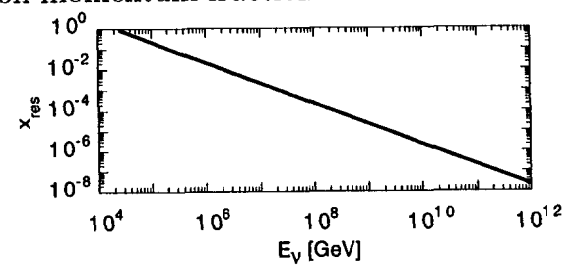

Slide 45

Implications for UHE neutrinos

For $E_\nu \gtrsim 10^6$ GeV, energy dependence of scalar resonance formation is similar to that of DIS.

- If HERA anomaly is an $e^+ +$ *valence quark* resonance, the effect on the νN interaction cross section is unlikely to grow large.
- If HERA is observing an $e^+ +$ *sea quark* resonance, then the cross section in νN interactions could become substantial at UHE.

Slide 46

Summary

In the absence of new physics,

- We can consider $\sigma(\nu_\ell N \to \ell + \text{anything})$ and $\sigma(\nu_\ell N \to \nu_\ell + \text{anything})$ "known," up to $E_\nu \approx 10^{15}$ eV.
- $\sigma_{\rm CC}$ and $\sigma_{\rm NC}$ can be predicted within a factor of 2 up to 10^{20} eV.
- Resonant $\bar{\nu}_e e$ scattering is dramatic in the neighborhood of $E_\nu \approx 6.3$ PeV.

The HERA high-Q^2 anomaly is unlikely to change interaction cross sections qualitatively.

In spite of lower AGN fluxes, a detector with an effective area $\gtrsim 0.1$ km^2 has great potential to open the study of UHE neutrino astronomy.

Slide 47

Pure Speculation . . .

(metaphorically related to string duality)

J. Bordes, *et al.* hep-ph/9705463

- Interpret $E \gtrsim 10^{20}$ eV air showers as FCNC νN interactions mediated by massive (~ 100 TeV) gauge bosons related to fermion generations. These "dual gluons" have gauge coupling $\tilde{g}$ such that

$$\tilde{g}g = 4\pi.$$

- Dual gluon contribution to $\sigma(\nu N)$ rises linearly with energy, approaching 10^{-29} cm^2 for $E_\nu \approx 10^{20}$ eV.
- Resonant formation of the dual gluon may occur in $\bar{\nu}_e e$ interactions at $E_\nu \gtrsim 10^{20}$ eV, for $M_{\tilde{g}} \gtrsim 10$ TeV.

Slide 48

Thanks to . . .

Raj Gandhi
Hallsie Reno
Ina Sarcevic
Tao Han
Marcela Carena
Frank Sciulli

et merci aux Gentils Organisateurs!

Slide 49